CHIN. PHYS. LETT. Vol. 37, No. 3 (2020) 034204 **Express Letter**

Asymptotical Locking Tomography of High-Dimensional Entanglement *

Ling-Jun Kong(孔令军)[1,2], Rui Liu(刘瑞)[3], Wen-Rong Qi(齐文荣)[3], Zhou-Xiang Wang(王周祥)[3], Shuang-Yin Huang(黄双印)[3], Chenghou Tu(涂成厚)[3], Yongnan Li(李勇男)[3]**, Hui-Tian Wang(王慧田)[1,2]**

[1]*National Laboratory of Solid State Microstructures, Nanjing University, Nanjing 210093*

[2]*Collaborative Innovation Center of Advanced Microstructures, Nanjing University, Nanjing 210093*

[3]*Key Laboratory of Weak-Light Nonlinear Photonics and School of Physics, Nankai University, Tianjin 300071*

(Received 10 February 2020)

High-dimensional (HD) entanglement provides a very promising way of transcending the limitations of the two-dimensional entanglement between qubits for increasing channel capacity in many quantum protocols. In the pursuit of capitalizing on the HD entangled states, one of the central issues is to unambiguously and comprehensively quantify and reconstruct them. The full quantum state tomography is a unique solution, but it is undesirable and even impractical because the measurements increase rapidly in d^4 for a bipartite d-dimensional quantum state. Here we present a very efficient and practical tomography method—asymptotical locking tomography (ALT), which can harvest full information of bipartite d-dimensional entangled states by very few measurements less than $2d^2$ only. To showcase the validity and reasonableness of our ALT, we carry out the test with the two-photon spin-orbital angular momentum hyperentangled states in a four-dimensional subspace. Besides high-efficiency and practicality, our ALT is also universal and can be generalized into multipartite HD entanglement and other quantum systems.

PACS: 42.30.Va, 42.30.−d, 42.65.Lm DOI: 10.1088/0256-307X/37/3/034204

Quantum entanglement is a fundamental quantum phenomenon and has formed the cornerstone of quantum information.[1,2] Entanglement can be generated in different physical systems such as photons,[3] atoms,[4] ions[5] and superconducting circuits.[6,7] The study on entanglement in two-dimensional photon systems has been quite mature. For example, the polarization-entangled Bell states of photons have been produced from spontaneous parametric down conversion (SPDC),[8] verified by full quantum state tomography,[9] transformed by wave plates,[8] and discriminated by nonlinear optics[10] or hyperentanglement.[11,12] Polarization entanglement has been applied into quantum dense coding,[12,13] quantum teleportation,[14] quantum key distribution,[15] and entanglement swapping.[16] Due to the limitation of dimension, the quantum protocols based on the polarization-entangled Bell states is limited to 2 bits for a single qubit. High-dimensional entanglement is the most promising way of transcending the limitation, because it allows more information to be encoded per particle and offers improved robustness against sophisticated eavesdropping attacks with respect to the two-dimensional one.[17,18]

High-dimensional (HD) entanglement can be achieved with different degrees of freedom such as orbital angular momentum (OAM),[19] energy-time[20] and frequency modes.[21] To capitalize on the HD entangled states, the prerequisite is to quantify them explicitly. Hence, several quantum state tomography methods have been presented, such as full quantum state tomography (F-QST),[9,22] mutually unbiased bases quantum state tomography (MUB-QST),[23,24] and symmetric informationally complete positive operator-valued quantum state tomography.[25] For bipartite entangled state with each particle having d-dimension, the measurements required in the above methods dramatically increase in d^4, making them impractical for the HD entanglement. This will strongly mitigate possible advantages and practical applications of HD entanglement. An idea, which greatly reduces the measurements to $2d^2$, can certify only effective dimension of HD entanglement.[26] Therefore, there is still a formidable challenge how to find an efficient and practical strategy, which not only dramatically reduces the measurements, but also harvest the full information of HD entangled state, like the traditional F-QST.

Here we present a very efficient and practical method—asymptotical locking tomography (ALT), which can acquire the full information of bipartite entangled state with each particle having d-dimension by measurements less than $2d^2$. The asymptotical locking process of our ALT is described as follows. We first select a set of orthogonal basis $\{|\phi_m^X\rangle\}$ (X represents particle A or B) as the first basis, then measure coincidence counts matrix $\boldsymbol{N}'$ to harvest the normalized coefficient matrix of the intended target entangled

*Supported by the National Key R&D Program of China under Grant Nos. 2017YFA0303800 and 2017YFA0303700, the National Natural Science Foundation of China under Grant Nos. 11534006, 91750202, 11774183 and 11674184, and the Collaborative Innovation Center of Extreme Optics.

**Corresponding author. Email: liyongnan@nankai.edu.cn; htwang@nju.edu.cn

state under the first global product basis $\{|\phi_m^X\rangle|\phi_n^X\rangle\}$. To further acquire the information of phases of the intended target entangled state, we construct another suitable basis $\{|\varphi_m^X\rangle\}$ as the second one and measure the coincidence counts matrix $\boldsymbol{N''}$ under the second global product basis $\{|\varphi_m^X\rangle|\varphi_n^X\rangle\}$. The second basis $\{|\varphi_m^X\rangle\}$ is constructed by using $\{|\phi_m^X\rangle\}$ and a certain criterion defined by $\boldsymbol{N'}$. Then, pure bipartite quantum states in any dimension can be unambiguously certified and faithfully reconstructed under two global product bases, without resorting to inefficient traditional full state tomography. In particular, we also develop the ALT theory for the mixed state caused by the dephased maximally entangled state.

Pre-locking the target state.—One of the main tasks of quantum state tomography is to determine whether a quantum state prepared in lab is the intended one and how much is the difference between them. Therefore, for the first step, we should select a set of suitable orthogonal basis $\{|\phi_m^X\rangle\}$ and then carry out d^2 local projective measurements under the first global product basis $\{|\phi_m^X\rangle|\phi_n^X\rangle\}$. We will have a general understanding of the state prepared in lab, which is described by a density matrix ρ. With the coincidence counts matrix $\boldsymbol{N'}$ measured under $\{|\phi_m^X\rangle|\phi_n^X\rangle\}$, we can obtain $\lambda_{mn} = \sqrt{\langle\phi_m^A|\langle\phi_n^B|\rho|\phi_m^A\rangle|\phi_n^B\rangle} = \sqrt{N'_{mn}/\sum_{m,n}N'_{mn}}$, where $\{\lambda_{mn}\}$ is the normalized coefficient matrix of the state prepared in lab under $\{|\phi_m^A\rangle|\phi_n^B\rangle\}$. Here we consider two cases: pure entangled state and mixed state. (i) For a pure entangled state, if the first basis is well selected to be a Schmidt basis, the number of nonzero λ_{mn} is only d.[26,27] Without loss of generality, we can set $\lambda_{mn}|_{m\neq n} = 0$. The density matrix ρ should be

$$\rho = |\Phi\rangle\langle\Phi|, \quad |\Phi\rangle = \sum\nolimits_m \lambda_m e^{i\theta_m}|\phi_m^A\rangle|\phi_n^B\rangle, \quad (1)$$

where $\lambda_m = \sqrt{N'_m/\sum_m N'_m}$, N'_m is the abbreviation of N'_{mm}, and $\theta_m \in [0,\pi]$ is the phase of $|\phi_m^A\rangle|\phi_n^B\rangle$. (ii) For a mixed state $|\Phi\rangle$ obtained by dephasing, its density matrix ρ should be[28]

$$\rho(p) = p|\Phi\rangle\langle\Phi| + (1-p)\sum\nolimits_m \lambda_m^2|\phi_m^A\rangle|\phi_m^B\rangle\langle\phi_m^A|\langle\phi_m^B|, \quad (2)$$

where $p \in [0,1]$ is the visibility, which can also characterize the noise level.

Pure state: acquiring the phase information.—To acquire the phases, we need to construct the second basis $\{|\varphi_m^X\rangle\}$ by the first basis $\{|\phi_m^X\rangle\}$ with a transformation matrix. To search for the desired transformation matrix, we introduce a criterion matrix $\boldsymbol{C}$ defined by the measured $\boldsymbol{N'}$

$$C_{kl} = \left|\sum\nolimits_{m=1}^d \lambda_m \tilde{T}_{mk}^\dagger \tilde{T}_{ml}^\dagger e^{i\beta_m}\right|^2, \quad (3)$$

where C_{kl} is an element of $\boldsymbol{C}$ and $\tilde{T}_{kl}$ is an element of transformation matrix $\tilde{\boldsymbol{T}}$. We then define a criterion

$$\boldsymbol{C}(\tilde{\boldsymbol{T}},\{\beta_m\}) = \boldsymbol{C}(\tilde{\boldsymbol{T}},\{\beta'_m\}), \quad \text{iff } \{\beta_m\} = \{\beta'_m\}, \quad (4)$$

which means that for the desired transformation matrix, $\boldsymbol{C}$ for different $\{\beta_m\}$ must be non-degenerate. During the optimal search with the two-fold nested loops ($\tilde{\boldsymbol{T}}$ as the outer loop and $\{\beta_m\}$ as the inner loop, see Fig. S1 and the Supplemental Material for details). If the above criterion is satisfied, the searched $\tilde{\boldsymbol{T}}$ will be the transformation matrix $\boldsymbol{T}$ we desired. Then $|\varphi_m^X\rangle$ can be written as

$$|\varphi_m^X\rangle = \sum\nolimits_{n=1}^d T_{mn}|\phi_n^X\rangle, \quad X = A \text{ or } B, \quad (5)$$

where T_{mn} are elements of matrix $\boldsymbol{T}$. One should point out that $\{|\varphi_m^X\rangle\}$ is normalized but not necessarily orthogonal.

We perform the measurements under the second global product basis $\{|\varphi_m^A\rangle|\varphi_n^B\rangle\}$ to obtain the coincidence counts matrix $\boldsymbol{N''}$. With $\boldsymbol{T}$, $\boldsymbol{N'}$ and $\boldsymbol{N''}$, we can build a set of nonlinear equations as follows:

$$\left|\sum\nolimits_{m=1}^d \Gamma_{mkl}^\dagger e^{i\theta_m}\right|^2 = N''_{kl}/N''_C, \quad (6)$$

where $\Gamma_{mkl}^\dagger = \lambda_m T_{mk}^\dagger T_{ml}^\dagger$, N''_C is the normalized coefficient and N''_{kl} is an element of $\boldsymbol{N''}$. Clearly, $\boldsymbol{N''}$ is a symmetric matrix ($N''_{kl} = N''_{lk}$), so we need to measure experimentally only $(d^2+d)/2$ independent elements of $\boldsymbol{N''}$ instead of all the d^2 elements under $\{|\varphi_m^A\rangle|\varphi_n^B\rangle\}$. For $\{\theta_m\}$, only the relative phases are important, so we can set $\theta_1 = 0$. Clearly, Eq. (6) contains $(d^2+d)/2$ sub-equations, but only $(d-1)$ sub-equations are independent. In our real processing, therefore we need to select only $(d-1)$ sub-equations from Eq. (6) for solving $(d-1)$ unknown phases $\{\theta_m\}_{m\geq 2}$. To reduce error, however, the selection must follow a rule that the selected $(d-1)$ sub-equations should contain the $(d-1)$ largest elements among the measured coincidence matrix $\boldsymbol{N''}$. One should point out that to achieve the tomography of any pure HD entangled state, our ALT method carries out the total measurements $d^2 + (d^2+d)/2 < 2d^2$ only.

Mixed state: acquiring the phase information and the visibility.—In this case, the criterion for searching the desired transformation matrix $\boldsymbol{T}$ in Eq. (4) is still valid. The coincidence counts matrix $\boldsymbol{N''}$ can also be measured under the global product basis $\{|\varphi_m^A\rangle|\varphi_n^B\rangle\}$ obtained by Eq. (5). With $\boldsymbol{T}$, $\boldsymbol{N'}$ and $\boldsymbol{N''}$, a set of nonlinear equations can be built as

$$p\left|\sum_{m=1}^d \Gamma_{mkl}^\dagger e^{i\theta_m}\right|^2 + (1-p)\sum_{m=1}^d |\Gamma_{mkl}^\dagger|^2 = N''_{kl}/N''_C. \quad (7)$$

As mentioned above, we still set $\theta_1 = 0$ and only $(d-1)$ sub-equations among $(d^2+d)/2$ sub-equations

in Eq. (7) are independent. Due to the presence of the visibility p, the $(d-1)$ independent sub-equations in Eq. (7) are not enough to determine the $(d-1)$ unknown phases $\{\theta_m\}_{m\geq 2}$ and the visibility p. In principle, only one independent sub-equation (the dth independent one) is built again, we can determine $\{\theta_m\}_{m\geq 2}$ and p completely. Therefore, we need to construct the third basis $\{|\psi_m^X\rangle\}$ and then to measure coincidence counts matrix $\boldsymbol{N}'''$ under this basis. $\{|\psi_m^X\rangle\}$ is defined as

$$|\psi_m^X\rangle = \sum_{n=1}^{d} T'_{mn}|\phi_n^X\rangle, \quad X = A \text{ or } B, \tag{8}$$

where T'_{mn} are elements of transformation matrix $\boldsymbol{T}'$, which also satisfies the criterion in Eq. (4).

Similarly, based on the coincidence counts $\boldsymbol{N}'''$ under the third product basis $\{|\psi_m^A\rangle|\psi_n^B\rangle\}$, a new set of nonlinear equations can be built as

$$p\Big|\sum_{m=1}^{d} \Gamma'^{\dagger}_{mkl} e^{i\theta_m}\Big|^2 + (1-p)\sum_{m=1}^{d}|\Gamma'^{\dagger}_{mkl}|^2 = N'''_{kl}/N'''_C, \tag{9}$$

where $\Gamma'^{\dagger}_{mkl} = \lambda_m T'^{\dagger}_{mk} T'^{\dagger}_{ml}$, N'''_C is the normalized coefficient, and N'''_{kl} is an element of $\boldsymbol{N}'''$. In fact, to build the dth independent sub-equation, we do not need to measure all the $(d^2+d)/2$ independent elements in $\boldsymbol{N}'''$. We only need to measure two larger matrix elements in $\boldsymbol{N}'''$, which are defined as N'''_{kl} and N'''_{uv}. Thus, with Eq. (9), we can build the dth independent sub-equation as

$$\frac{p\Big|\sum_{m=1}^{d} \Gamma'^{\dagger}_{mkl} e^{i\theta_m}\Big|^2 + (1-p)\sum_{m=1}^{d}|\Gamma'^{\dagger}_{mkl}|^2}{p\Big|\sum_{m=1}^{d} \Gamma'^{\dagger}_{muv} e^{i\theta_m}\Big|^2 + (1-p)\sum_{m=1}^{d}|\Gamma'^{\dagger}_{muv}|^2} = \frac{N'''_{kl}}{N'''_{uv}}. \tag{10}$$

Finally, by solving the selected $(d-1)$ equations in (7) and (10) together, we can acquire all $\{\theta_m\}$ and p completely. Clearly, compared with the pure state, only a few measurements need to be increased for the tomography of the mixed HD entangled state.

Experiment.—As shown in Fig. 1(a), we select maximally hyperentangled state $|\Phi_1\rangle \propto (|H^A\rangle|H^B\rangle + |V^A\rangle|V^B\rangle)\otimes|\Psi^+_{\rm OAM}\rangle$ as an intended target spin-OAM state, with $|\Psi^+_{\rm OAM}\rangle \propto (|+1^A\rangle|-1^B\rangle + |-1^A\rangle|+1^B\rangle)$. The preferred orthogonal bases are $|\nu_1\rangle = |H,+1\rangle$, $|\nu_2\rangle = |V,+1\rangle$, $|\nu_3\rangle = |V,-1\rangle$, and $|\nu_4\rangle = |H,-1\rangle$, where $|H,l\rangle$ ($|V,l\rangle$) stands for a state of photon with horizontal (vertical) polarization and an OAM of $l\hbar$. As shown in Fig. 1(b), we carry out the projective operations under the basis $\{|\nu_m\rangle\}$ with two HWPs (half wave plates), two QWPs (quarter wave plates), a 1/2-order q-plate,[29,30] a PBS (polarizing beam splitter), and an SMF (single mode fibre). For the detailed projective evolutions one can see Fig. S2 and the Supplemental Material.

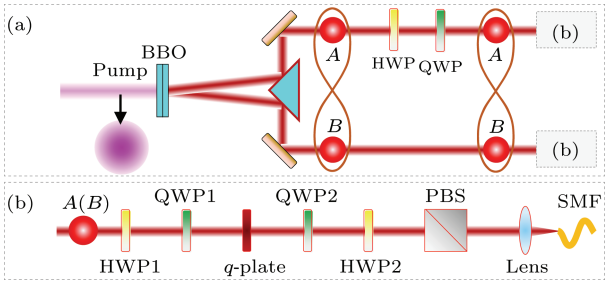

Fig. 1. Experimental setup. (a) Entanglement source. A fundamental Gaussian fs laser pumps two 0.6-mm-thick BBO crystals with optic axes aligned in perpendicular planes. A four-dimensional (4D) spin-OAM hyperentangled state is generated by the type-I SPDC. An unitary operation on photon-A can transform the initial 4D hyperentangled state $|\Phi_1\rangle$ into $|\Phi_2\rangle$, $|\Phi_3\rangle$ or $|\Phi_4\rangle$. (b) Scheme of projective measurement under the first basis $\{|\phi_m^{A/B}\rangle\}$ and second basis $\{|\varphi_m^{A/B}\rangle\}$ $(m = 1, 2, 3, 4)$.

We then measure the coincidence counts matrix $\boldsymbol{N}$ under the global product basis $\{|\nu_m\rangle|\nu_n\rangle\}$ in Fig. 2(a1). $\boldsymbol{N}$ is a non-diagonal matrix. For the convenience in the handling problem, we select the coincidence counts matrix $\boldsymbol{N}'$ under the first global product basis $\{|\phi_m^A\rangle|\phi_n^B\rangle\}$ to be a diagonal one. Therefore, the first orthogonal basis $\{|\phi_m^X\rangle\}$ by $\{|\nu_m\}$ should be define as $|\phi_1^A\rangle = |\nu_1\rangle$, $|\phi_2^A\rangle = |\nu_2\rangle$, $|\phi_3^A\rangle = |\nu_3\rangle$, $|\phi_4^A\rangle = |\nu_4\rangle$; $|\phi_1^B\rangle = |\nu_4\rangle$, $|\phi_2^B\rangle = |\nu_3\rangle$, $|\phi_3^B\rangle = |\nu_2\rangle$, $|\phi_4^B\rangle = |\nu_1\rangle$. $\boldsymbol{N}'$ in Fig. 2(a2) comes from $\boldsymbol{N}$ in Fig. 2(a1) without resorting to remeasurement under the first global product basis $\{|\phi_m^A\rangle|\phi_n^B\rangle\}$. Thus, we can write the preliminary result of tomography for the state generated in lab as $|\Phi_1^T\rangle = \sum_{m=1}^{4}\lambda_m e^{i\theta_m}|\phi_m^A\rangle|\phi_m^B\rangle$, where $\lambda_m = \sqrt{N'_m/\sum_m N'_m}$, and N'_m is a diagonal element of $\boldsymbol{N}'$. Following the criterion in Eq. (4), we find the desired $\boldsymbol{T}$ to construct the second basis as

$$\begin{bmatrix}|\varphi_1^X\rangle\\|\varphi_2^X\rangle\\|\varphi_3^X\rangle\\|\varphi_4^X\rangle\end{bmatrix} \propto \boldsymbol{T}\begin{bmatrix}|\phi_1^X\rangle\\|\phi_2^X\rangle\\|\phi_3^X\rangle\\|\phi_4^X\rangle\end{bmatrix}, \quad \boldsymbol{T} = \frac{1}{2}\begin{bmatrix}1 & 1 & 1 & -1\\ 1 & 1 & -1 & 1\\ 1 & -1 & 1 & 1\\ -1 & 1 & 1 & 1\end{bmatrix}. \tag{11}$$

The arrangement for performing the projective operations of basis $\{|\varphi_m^X\rangle\}$ is the same one for $\{|\nu_m\rangle\}$ (see the Supplemental Material for details).

We measure the coincidence counts matrix $\boldsymbol{N}''$ under the global product basis $\{|\varphi_m^A\rangle|\varphi_n^B\rangle\}$ in Fig. 2(a3). Substituting $\boldsymbol{N}'$, $\boldsymbol{N}''$, $|\Phi_1^T\rangle$ and Eq. (11) into Eq. (6), we can harvest all the phases $\{\theta_m\}$ and realize the full quantum state tomography of the 4D entangled state. We calculate the density matrix $\rho_1^T = |\Phi_1^T\rangle\langle\Phi_1^T|$ in Fig. 2(a4), suggesting that the state generated in lab is indeed close to the intended target state $|\Phi_1\rangle$ in Fig. 2(a5). We also estimate the fidelity to be $F(\rho_1^T, \Phi_1) = \mathrm{Tr}(|\Phi_1\rangle\langle\Phi_1|\rho_1^T) = (90.63 \pm 0.40)\%$.

To test our ALT again, we carry out the measurements of other maximally hyperentangled spin-OAM states. By the unitary operations with an HWP and a QWP on photon-A, we can prepare the 4D maximally

entangled state $|\Phi_2\rangle$ from $|\Phi_1\rangle$,

$$|\Phi_2\rangle \propto (|H^A\rangle|V^B\rangle - |V^A\rangle|H^B\rangle) \otimes |\Psi^+_{\rm OAM}\rangle. \quad (12)$$

For the ALT measurement of the intended target state $|\Phi_2\rangle$ produced in lab, the procedure is very similar to that of $|\Phi_1\rangle$. The preferred orthogonal bases are still $\{|\nu_m\rangle\}$. We measure the coincidence counts matrix $\boldsymbol{N}$ under the global product basis $\{|\nu_m\rangle|\nu_n\rangle\}$ in Fig. 2(b1). Different from $|\Phi_1\rangle$, the first orthogonal bases $\{|\phi^X_m\rangle\}$ for $|\Phi_2\rangle$ are selected as $|\phi^A_1\rangle = |\nu_1\rangle$, $|\phi^A_2\rangle = |\nu_2\rangle$, $|\phi^A_3\rangle = |\nu_3\rangle$, $|\phi^A_4\rangle = |\nu_4\rangle$; $|\phi^B_1\rangle = |\nu_3\rangle$, $|\phi^B_2\rangle = |\nu_4\rangle$, $|\phi^B_3\rangle = |\nu_1\rangle$, $|\phi^B_4\rangle = |\nu_2\rangle$ to obtain directly the diagonal coincidence counts matrix $\boldsymbol{N}'$ under the global product bases $\{|\phi^A_m\rangle|\phi^B_n\rangle\}$ in Fig. 2(b2) from $\boldsymbol{N}$ in Fig. 2(b1). The second basis $\{|\varphi^X_m\rangle\}$ can be constructed from $\{|\phi^X_m\rangle\}$ by the same $\boldsymbol{T}$ in Eq. (11). We measure the coincidence counts matrix $\boldsymbol{N}''$ under the global product bases $\{|\varphi^A_m\rangle|\varphi^B_n\rangle\}$ in Fig. 2(b3). Finally, we harvest the ALT result $|\Phi^T_2\rangle$ for the intended target state $|\Phi_2\rangle$ and the density matrix $\rho^T_2 = |\Phi^T_2\rangle\langle\Phi^T_2|$ in Fig. 2(b4). The result shows that the entangled state produced in lab is close to the intended target state $|\Phi_2\rangle$ in Fig. 2(b5). The ALT results of other two maximally hyperentangled states ($|\Phi_3\rangle$ and $|\Phi_4\rangle$) can be found from Fig. S3 in the Supplemental Material. All the ALT results prove our witness.

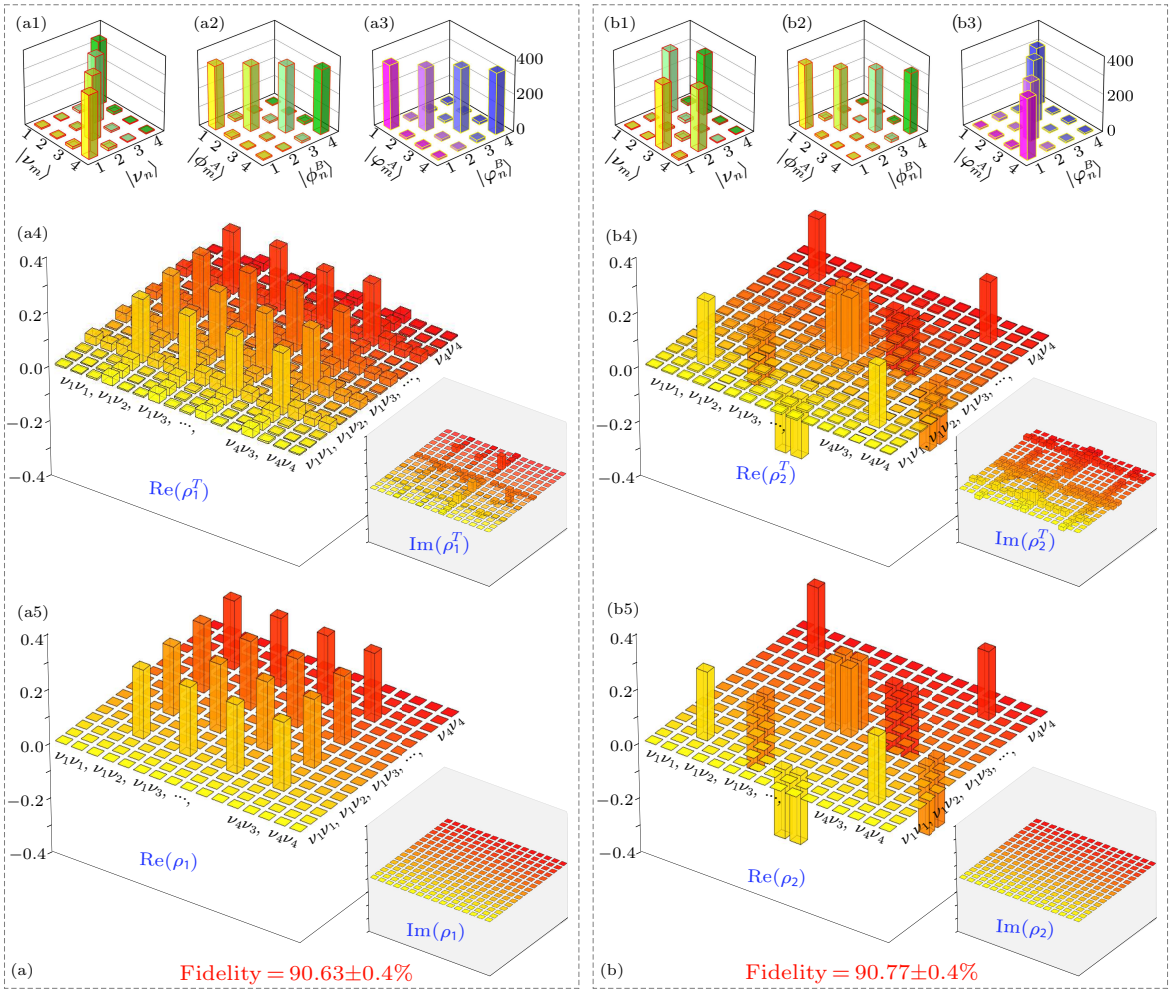

Fig. 2. Experimental data and reconstructed density matrices for the spin-OAM hyperentangled states. (a) Spin-OAM hyperentangled state $|\Phi_1\rangle$. (b) Spin-OAM hyperentangled state $|\Phi_2\rangle$. Coincidence counts for the intended target state $|\Phi_1\rangle$ under the global product bases of $\{|\nu_m\rangle|\nu_n\rangle\}$ (a1), the first basis $\{|\phi^A_m\rangle|\phi^B_n\rangle\}$ (a2), and the second basis $\{|\varphi^A_m\rangle|\varphi^B_n\rangle\}$ (a3). Here (a4) and (a5) are experimentally and theoretically reconstructed density matrices, respectively. Similar to (a1)–(a5), (b1)–(b5) show the results for the intended target state $|\Phi_2\rangle$.

Discussion.—We provide a clear physical picture to gain insight into our ALT (Fig. 3). The selection of first basis is important and should follow certain rules. (i) The first basis must be orthogonal and complete and (ii) we should consider the entangled degrees of freedom and spatial modes of states. The background of readily available knowledge about the interested quantum system provides us some hints to narrow the choice of the first basis. For the polarized entanglement, the first basis can be selected as $\{|H\rangle, |V\rangle\}$ (or $\{|H\rangle + |V\rangle, |H\rangle - |V\rangle\}$); for the OAM entangled states, the first basis can be selected as $\{|l\rangle\}$

with the Laguerre–Gaussian modes. For the spin-OAM hyperentangled states, we prefer the first basis to be $\{|H,l\rangle|V,l\rangle\}$. The choice of suitable first basis reduces the searching scope of the intended target state within the area surrounded by the black ellipse. The measured coincidence counts matrix $\boldsymbol{N}'$ under the first basis greatly narrows the searching scope into the area surrounded by the blue ellipse. The construction of the second basis is mainly restrained by the criterion matrix $\boldsymbol{C}$ related to the measured $\boldsymbol{N}'$. Clearly, the measured $\boldsymbol{N}'$ acts as a limitation or feedback to optimize the construction of the second basis. We carry out the coincidence measurements under the second global product basis to obtain the coincidence counts matrix $\boldsymbol{N}''$. By $\boldsymbol{N}''$, we can acquire the accurate phase information and finally identify the entangled state produced in lab (red ellipse), which is very close to the intended target entangled state (green ellipse). Such an "asymptotical locking" process plays an indispensable role in drastically reducing the measurements. By contrast, no criterion is used for constructing the second base (tilted base) in Ref. [26], which leads to the situation that they can only certify effective entangled dimension and fidelity of HD entangled state but cannot provide the full quantum state information.

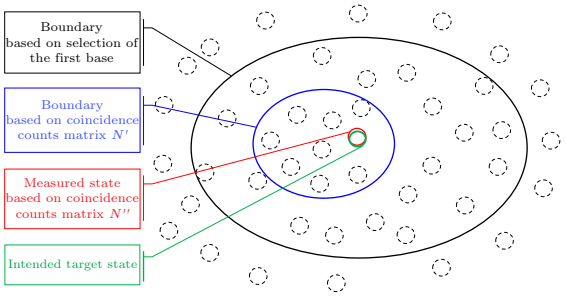

Fig. 3. ALT—Witnessing HD entanglement with two bases. Every potential target state is in a subspace of the infinite Hilbert space, which is composed of any available degree of freedom. Range of black ellipse is a subspace limited by the particles and degrees of freedom used in a specific experiment. The coincidence counts measured with the first base can give the boundary of blue ellipse. When the second base is properly selected, measured coincidence counts can narrow the border to the red ellipse. In principle, only the target state locates in the red ellipse. The green ellipse represents the intended target state. Due to the presence of noise, the red ellipse and the green ellipse do not completely coincide, which implies that the fidelity can not reach 100%.

For a d-dimensional bipartite entangled state, our ALT requires measurements $<2d^2$, which is much less than $\sim d^4$ of F-QST[9] and MUB-QST.[23,24] When $d=10$, our ALT needs 155 measurements only, while F-QST and MUB-QST require $\sim 10^4$ measurements. Compressed sensing technique used in the quantum state tomography[31,32] dramatically reduces the measurements, but they are still higher than our ALT.

A more practical method should not only be able to high-efficiently diagnose the quality of the prepared HD entangled light source, but also provide a guidance for optimizing the entangled source. Our strategy meets indeed such a pursuit. For instance, the initially produced entangled state in lab deviates from our intended target state [see Fig. S(4a)]. The analysis based on our ALT result tells us that HWP in path-A is not well aligned. After fine adjusting HWP, the entangled state is greatly optimized [see Fig. S(4b) and the Supplemental Material for details].

In conclusion, in the pursuit of capitalizing on the HD entangled states, one of the central issues is to unambiguously and comprehensively quantify and reconstruct them. The F-QST provides a solution, but it is too inefficient and even is impractical for fully diagnosing the HD entangled state. Our ALT needs to carry out only $d^2+(d^2+d)/2<2d^2$ measurements much less than the d^4 required ones for the standard F-QST, but full information of the d-dimensional entanglement can be still harvested to unambiguously certify and faithfully reconstruct the intended entangled states. Our ALT is the most efficient and practical method for tomography of the HD entangled states so far. It is valid for not only the pure HD entangled state but also the mixed state (dephased maximally entangled state). In addition, our ALT method can be generalized into multipartite HD entanglement with multi-degree of freedom (see the Supplemental Material) and other quantum systems. Our ALT method should be a great advance to promote the practical applications of HD entangled states.

References

[1] Schrödinger E 1935 *Naturwissenschaften* **23** 823
[2] Trimmer J D 1980 *Proc. Am. Philos. Soc.* **124** 323
[3] Wang X L, Chen L K, Li W, Huang H L, Liu C, Chen C, Luo Y H, Su Z E, Wu D, Li Z D, Lu H, Hu Y, Jiang X, Peng C Z, Li L, Liu N L, Chen Y A, Lu C Y and Pan J W 2016 *Phys. Rev. Lett.* **117** 210502
[4] Anderson B E, Sosa-Martinez H, Riofrío C A, Deutsch I H and Jessen P S 2015 *Phys. Rev. Lett.* **114** 240401
[5] Lanyon B P, Zwerger M, Jurcevic P, Hempel C, Dür W, Briegel H J, Blatt R and Roos C F 2014 *Phys. Rev. Lett.* **112** 100403
[6] Kelly J, Barends R, Fowler A G, Megrant A, Jeffrey E, White T C, Sank D, Mutus J Y, Campbell B, Chen Y, Chen Z, Chiaro B, Dunsworth A, Hoi I C, Neill C, O'Malley P J J, Quintana C, Roushan P, Vainsencher A, Wenner J, Cleland A N and Martinis J M 2015 *Nature* **519** 66
[7] Kumar K S, Vepsäläinen A, Danilin S and Paraoanu G S 2016 *Nat. Commun.* **7** 10628
[8] Kwiat P G, Mattle K, Weinfurter H, Zeilinger A, Sergienko A V and Shih Y H 1995 *Phys. Rev. Lett.* **75** 4337
[9] James D F V, Kwiat P G, Munro W J and White A G 2001 *Phys. Rev. A* **64** 052312
[10] Kim Y H, Kulik S P and Shih Y H 2001 *Phys. Rev. Lett.* **86** 1370
[11] Schuck C, Huber G, Kurtsiefer C and Weinfurter H 2006 *Phys. Rev. Lett.* **96** 190501
[12] Barreiro J T, Wei T C and Kwiat P G 2008 *Nat. Phys.* **4**

282
[13] Williams B P, Sadlier R J and Humble T S 2017 *Phys. Rev. Lett.* **118** 050501
[14] Bouwmeester D, Pan J W, Mattle K, Eibl M, Weinfurter H and Zeilinger A 1997 *Nature* **390** 575
[15] Lo H K and Chau H F 1999 *Science* **283** 2050
[16] Pan J W, Bouwmeester D, Weinfurter H and Zeilinger A 1998 *Phys. Rev. Lett.* **80** 3891
[17] Wang C, Deng F G, Li Y S, Liu X S and Long G L 2005 *Phys. Rev. A* **71** 044305
[18] Huber M and Pawlowski M 2013 *Phys. Rev. A* **88** 032309
[19] Krenn M, Malik M, Erhard M and Zeilinger A 2017 *Philos. Trans. R. Soc. A* **375** 20150442
[20] Martin A, Guerreiro T, Tiranov A, Designolle S, Fröwis F, Brunner N, Huber M and Gisin N 2017 *Phys. Rev. Lett.* **118** 110501
[21] Bernhard C, Bessire B, Feurer T and Stefanov A 2013 *Phys. Rev. A* **88** 032322
[22] Thew R T, Nemoto K, White A G and Munro W J 2002 *Phys. Rev. A* **66** 012303
[23] Adamson R B A and Steinberg A M 2010 *Phys. Rev. Lett.* **105** 030406
[24] Giovannini D, Romero J, Leach J, Dudley A, Forbes A and Padgett M J 2013 *Phys. Rev. Lett.* **110** 143601
[25] Bent N, Qassim H, Tahir A A, Sych D, Leuchs G, Sanchez-Soto L L, Karimi E and Boyd R W 2015 *Phys. Rev. X* **5** 041006
[26] Bavaresco J, Valencia N H, Klöckl C, Pivoluska M, Erker P, Friis N, Malik M and Huber M 2018 *Nat. Phys.* **14** 1032
[27] Malik M, Erhard M, Huber M, Krenn M, Fickler R and Zeilinger A 2016 *Nat. Photon.* **10** 248
[28] Erker P, Krenn M and Huber M 2017 *Quantum* **1** 22
[29] Marrucci L, Manzo C and Paparo D 2006 *Phys. Rev. Lett.* **96** 163905
[30] Kong L J, Liu R, Qi W R, Wang Z X, Huang S Y, Wang Q, Tu C, Li Y and Wang H T 2019 *Sci. Adv.* **5** eaat9206
[31] Gross D, Liu Y K, Flammia S T, Becker S and Eisert J 2010 *Phys. Rev. Lett.* **105** 150401
[32] Wang J, Paesani S, Ding Y, Santagati R, Skrzypczyk P, Salavrakos A, Tura J, Augusiak R, Mančinska L, Bacco D, Bonneau D, Silverstone J W, Gong Q H, Acín A, Rottwitt K, Oxenløwe L K, O'Brien J L, Laing A and Thompson M G 2018 *Science* **360** 285